Graphical Abstract

A study of the supramolecular assembly formed by cucurbit[7]uril and 4-cyanophenol

Zhi-Chao Yu [a], Yun Lu [a], Jie Zhao [a], Jing-Jing Dai [a], Guo-Rong Chen [a], Pei-Hui Shan [a], Carl Redshaw [b], Zhu Tao [a], Xin Xiao [a, *]

[a] *Key Laboratory of Macrocyclic and Supramolecular Chemistry of Guizhou Province, Guizhou University, Guiyang 550025, China*
[b] *Chemistry, School of Natural Sciences, University of Hull, Hull HU6 7RX, U.K.*

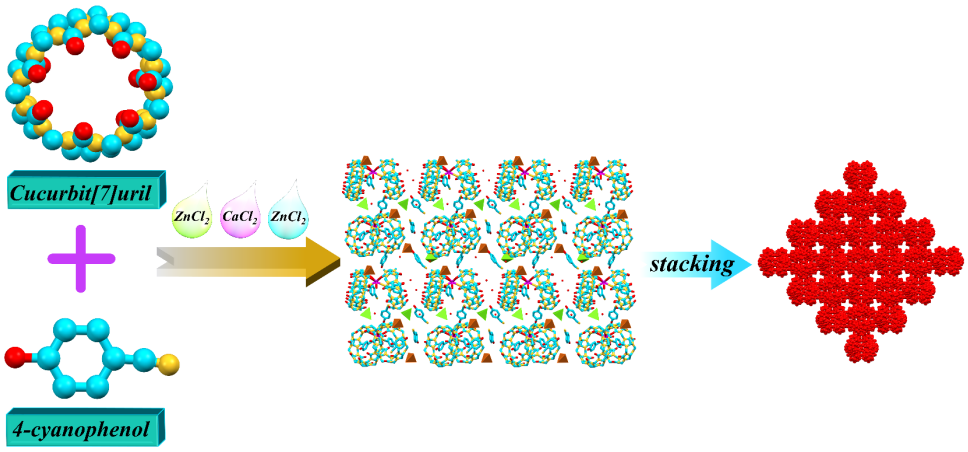

In this work, the binding interaction between 4-cyanophenol (4-CY) and cucurbit[7]uril has been studied and a Q[7]-based supramolecular framework was constructed in HCl solution.

A study of the supramolecular assembly formed by cucurbit[7]uril and 4-cyanophenol

Zhi-Chao Yu [a], Yun Lu [a], Jie Zhao [a], Jing-Jing Dai [a], Guo-Rong Chen [a], Pei-Hui Shan [a], Carl Redshaw [b], Zhu Tao [a], Xin Xiao [a, *]

[a] Key Laboratory of Macrocyclic and Supramolecular Chemistry of Guizhou Province, Guizhou University, Guiyang 550025, China
[b] Chemistry, School of Natural Sciences, University of Hull, Hull HU6 7RX, U.K.

ARTICLE INFO

Keywords:
Cucurbit[7]uril
4-Cyanophenol
Host-guest chemistry
Supramolecular assembly

ABSTRACT

The binding interaction between 4-cyanophenol (4-CY) and cucurbit[7]uril has been studied using ^{1}H NMR spectroscopy, UV-vis absorption spectroscopy, fluorescence spectroscopy and X-ray crystallography. The corresponding absorption and emission spectra obtained in aqueous solution revealed that Q[7] and 4-CY formed a 1:1 host-guest type complex. A single crystal structure was obtained by introducing $[ZnCl_4]^{2-}$ and Ca^{2+} as structural inducers, which revealed that 4-CY was connected to Q[7] or $[ZnCl_4]^{2-}$ anion *via* weak interactions such as hydrogen bonding, C-H···π, ion-dipole, to afford a Q[7]-based supramolecular framework. Interestingly, the framework exhibited a Chinese knot-like structure.

1. Introduction

Recently, host-guest complexation has gained increasing attention [1-3]. Cucurbit[*n*]urils (Q[*n*]s, n=5−8, 10 and 13−15), are a family of organic macrocyclic hosts that are derived from the condensation of glycoluril and formaldehyde [4-6]. They possess glycoluril units bridged by methylene groups, a hydrophobic pumpkin-shaped cavity, two ports filled with numerous carbonyl oxygen groups, and a positively charged outer surface [7-8]. On account of these structural features, Q[*n*]s are most commonly used in supramolecular chemistry, and advances have been made in host-guest chemistry [9-12] and coordination chemistry [13-15]. Remarkable aqueous host-guest chemistry is possible because of their selectivity and excellent capacity to include specific guests in solution [16-19]. The Q[*n*]s hydrophobic cavities contribute to their host-guest complexation, which can bond positively charged guest molecules to form host-guest complexes *via* non-covalent interactions [20–22]. There are macrocyclic confinement effects due to differing degrees of polymerization having cavities of different confined sizes. Meanwhile, the negatively charged Q[*n*]s carbonyl portals promote the coordination of metal cations to form coordination complexes through ion-dipole interactions [23–24]. In addition, the outer surface of Q[*n*]s can bond guest molecules to form Q[*n*]-outer-surface complexes by hydrogen bondings, C-H···π, π···π, and ion-dipole interactions [25]. Therefore, the use of Q[*n*]s as building blocks can provide a variety of Q[*n*]-based supramolecular frameworks (QSFs) [26-28]. The construction mode for the QSFs can be divided into self-induced, anion-induced or aromatic-induced [29-30]. The construction of QSFs with novel structures and specific functional properties may establish a new research direction in Q[*n*] chemistry.

4-Hydroxylbenzenitrile is an organic aromatic compound, commonly known as 4-cyanophenol (4-CY), which is an important fine organic chemical/raw material and a useful synthetic intermediate [31-32]. Its molecular structure contains an aromatic ring, a hydroxyl group and a cyano group, which can serve as C-H···π, π···π, interaction sites. The hydroxyl group is the hydrogen bond donor, and the cyano group is the hydrogen bond acceptor. It is an ideal guest molecule for host-guest complexation.

In this paper, one host-guest supramolecular structure comprising Q[7] and 4-cyanophenol was constructed. The binding interaction between 4-cyanophenol and Q[7] has been explored using ^{1}H NMR spectroscopy, UV-vis absorption spectroscopy, fluorescence spectroscopy and X-ray crystallography. Meanwhile, a Q[7]-based supramolecular framework was constructed by introducing $[ZnCl_4]^{2-}$ and Ca^{2+} as structural inducers in HCl solution. The structural characteristics are discussed in the crystal structure description.

2. Experimental section

2.1 Materials and methods

Q[7] was synthesized and purified in our laboratory as previously described [33]. The guest 4-cyanophenol and deuterium reagents were purchased from commercial suppliers and were used without further purification. Doubly-distilled water was always used in the experiments.

2.2 ^{1}H NMR spectroscopic measurement

The ^{1}H NMR spectra, including those for the titration experiments, were recorded on a JEOL JNM-ECZ400S 400 MHz NMR spectrometer at 298.15 K. Q[7] was incrementally added to a 50 mmol/L solution of 4-CY in D_2O. D_2O was used as a field-frequency lock, and chemical shifts were reported in ppm.

2.3 UV spectra and fluorescence measurements

To explore the interactions of Q[7]@4-CY complex, all UV-vis absorption was recorded with doubly-distilled water as the solvent on an Agilent 8453 UV-vis spectrophotometer (Hewlett Packard, California, USA). Fluorescence emission spectra were recorded on a VARIAN Cary Eclipse spectrofluorometer (Varian, Inc., Palo Alto, CA, USA). Stock solutions of Q[7] (1.0×10^{-3} M) were prepared using doubly-distilled water. The optimal UV-vis absorption concentration of 4-CY (3.0×10^{-5} M) and the optimal fluorescence emission concentration of 4-CY (5.0×10^{-5} M) were prepared by diluting the stock solutions. Then the concentration of 4-CY was fixed and the concentrations of Q[7] was constantly changed to maintain the molar ratio of $N_{Q[7]}/N_{4\text{-}CY}$ (0, 0.1, 0.2, ...). UV-vis spectra and fluorescence emission spectra were measured by the molar ratio method at 298.15 K. The Jobs plot method was used to further measure the inclusion ratio of the Q[7]@4-CY complex, a series of solutions to be measured satisfying $N_{4\text{-}CY}/N_{(Q[7]+4\text{-}CY)}$ = 0, 0.1, 0.2, 0.3 . . .1.0. The total concentration is constant ([Q[7] + [4-CY] = 3.0×10^{-5} M or 5.0×10^{-5} M).

2.4 Crystallization and structure determination

* Corresponding author.
E-mail address: gyhxxiaoxin@163.com

High-quality single crystals of Q[7]@4-CY suitable for X-ray diffraction were grown by slow evaporation. The structure was determined unambiguously by mean of X-ray diffraction analysis. A crystal with the appropriate transparency and size was picked under the microscope and mounted on the Bruker D8 VENTURE diffractometer, using graphite-monochromated Mo-Kα radiation (λ = 0.71073 Å) at 273(2) K, with φ and ω scan techniques. An empirical absorption correction was applied using the SADABS program [34]. The structure was solved with SHELXT, completed by subsequent difference Fourier syntheses, and refined on F^2 using all reflections with ShelXL-2018 [35] (full-matrix least-squares techniques) in the Olex2 package [36]. All non-hydrogen atoms in the whole structure were refined SQUEEZE routine of Platon was employed for complex because of the disordered solvent water molecules [37]. The detailed crystallographic data of the Q[7]@4-CY is listed in Table 1. The crystal data has been deposited in the Cambridge Crystal Data Center under accession number CCDC: 2211656. These data can be obtained free of charge *via* http://www.ccdc.cam.ac.uk/data request/cif.

2.5 Preparation of Q[7]@4-CY complex

The inclusion complex Q[7]@4-CY was prepared as follows: Q[7] powder (21.47 mg, 0.016 mmol) was put in a small vial where 5 mL of the HCl solution (5.0 mL, 6 mol/L) of 4-CY (7.60 mg, 0.064 mmol) and $ZnCl_2{\cdot}4H_2O$ (14.10 mg, 0.064 mmol), $CaCl_2{\cdot}6H_2O$ (13.05 mg, 0.059 mmol) were added. Then the mixture was stirred for 5 min and filtered. The mixture was stirred and heated until completely dissolved. The solution was placed in a ventilation area for slow evaporation over a period of about two weeks producing colorless crystals of complex Q[7]@4-CY.

3. Results and discussion

The interaction of 4-cyanophenol and Q[7] was explored using ^{1}H NMR spectroscopy, UV-vis spectroscopy, fluorescence spectroscopy and X-ray diffraction. ^{1}H NMR titration experiments were initially performed to monitor the host-guest binding behavior between 4-CY and Q[7]. As shown in Fig. 1, on gradual addition of Q[7] from 0 to 1.25 equivalents into the aqueous solution of 4-CY, both the signals of the two aromatic protons (H_a and H_b) underwent a gradual upfield shift on account of the shielding from the Q[7] cavity, indicating that 4-CY was completely encapsulated into the cavity of Q[7].

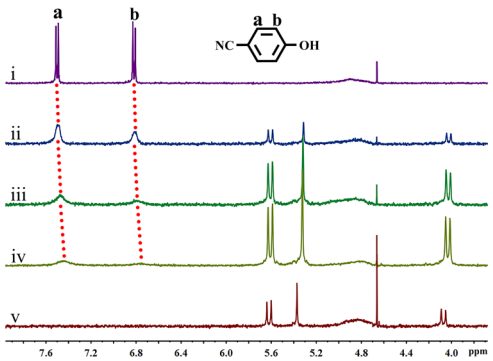

Fig. 1. ^{1}H NMR spectra of 4-CY (i) in the absence of Q[7]; (ii) in the presence of 0.10, (iii) 0.41, (iv) 1.10 equiv. of Q[7] and (v) neat Q[7] in D_2O at 20 °C

Next, the optical properties of the host-guest inclusion complex Q[7]@4-CY were explored using UV-vis spectroscopy and fluorescence spectroscopy. As shown in Fig. 2a, the major absorption peak of 4-CY decreased upon stepwise addition of Q[7] into aqueous solution of 4-CY, which is likely due to the 4-CY being in a different environment, that is, in the Q[7] cavity, compared with the unbound 4-CY. There is an inflection point for the absorbance intensity changes at 246 nm, which was approximately located at the amount of 1.0 equivalents Q[7] (Fig. 2b). A stoichiometric analysis (Jobs plot) also revealed a 1:1 binding stoichiometry for Q[7] and 4-CY (Fig. 2c).

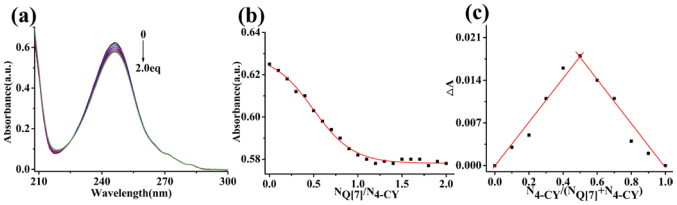

Fig. 2. (a) Changes in the UV-vis absorption spectra of 4-CY (3.0×10^{-5} M) in aqueous solution upon gradual of Q[7] (0~2.0 equiv); (b) changes in absorbance at 246 nm with various molar ratios of $N_{Q[7]}/N_{4\text{-}CY}$; (c) Jobs plot of Q[7] and 4-CY ([Q[7]] + [4-CY] = 3.0×10^{-5} M).

The fluorescence emission of 4-CY displays an emission peak at 308 nm in an aqueous solution when excited at 242 nm. As shown in Fig. 3a, the emission enhanced significantly upon stepwise addition of 0~2.0 equivalents Q[7] in the aqueous solution of 4-CY, which was attributed to the suppression of rotation and vibration of 4-CY when included in the finite cavity of the Q[7] [38]. It is worth noting that there is an obvious inflection point for the emission intensity changes at 308 nm, which was approximately located at the amount of 1.0 equivalents Q[7] (Fig. 3b). A Jobs plot further verified the stoichiometry of the host-guest inclusion complex (Fig. 3c). As a result, in the case of Q[7]@4-CY, the inclusion ability was confirmed by the corresponding absorption and emission spectra obtained in the aqueous solution of 4-CY. The binding constant value (Ka) calculated by the intensity-concentration fitting curve was (1.0224 ± 0.1980) × 10^4 M^{-1} (Fig. S1).

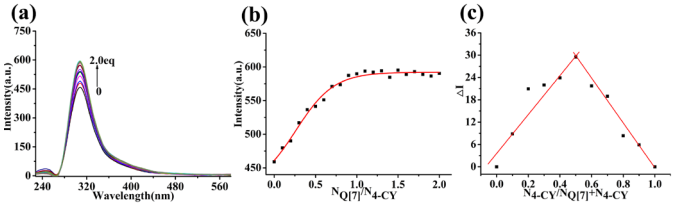

Fig. 3. (a) Changes in the fluorescence emission spectra of 4-CY (5.0×10^{-5} M) in aqueous solution upon gradual of Q[7] (0~2.0 equiv); (b) changes in emission at 308 nm with various molar ratios of $N_{Q[7]}/N_{4\text{-}CY}$; (c) Jobs plot of Q[7] and 4-CY ([Q[7]] + [4-CY] = 5.0×10^{-5} M).

In order to further obtain direct information about the binding interactions of 4-CY with Q[7], we also attempted to obtain single crystals by slow evaporation of the HCl solutions of Q[7] and 4-CY. By virtue of Q[*n*]s structural characteristics, Q[*n*]s have provided a focus for the development in research aimed at constructing various QSFs, including Q[*n*]-based supramolecular organic frameworks. As mentioned above, the QSF assembly process can be classified by three types: self-induced, anion-induced, or aromatic-induced. In view of this, we constructed a Q[7]-based QSF by using the aromatic ring properties of 4-CY and introducing $[ZnCl_4]^{2-}$ and Ca^{2+} as structural inducers in HCl solution. The structure and characteristics are discussed below.

The complex crystallizes in the tetragonal space group *P*-42_1c and the asymmetric unit contains one Ca^{2+} and one Q[7]@4-CY molecule, two coordinated water molecules and two protonated water molecules, along with two 4-CY molecules located outside the Q[7] host cavity and two $[ZnCl_4]^{2-}$ anions (Fig. 4a). As shown in Fig. 4b, the encapsulated 4-CY molecule runs through the cavity of the Q[7] host, and the angle between the plane where it is located and the plane established by the seven carbonyl oxygen atoms of the Q[7] host is 72.81°, and the N, O atoms of the 4-CY molecule are each in the plane established by the port carbonyl oxygen at both ends of the Q[7]. The Ca^{2+} coordinates with six oxygen atoms and two nitrogen atoms, with four oxygen atoms (O1, O2, $O1^i$, $O2^i$) which are derived from the carbonyl oxygen atoms at the ports of Q[7] in two adjacent Q[7]@4-CY, and the other two oxygen atoms (O18, $O18^i$) derived

from the coordinated water molecules. The two nitrogen atoms (N29, N29^{i}) are derived from the cyanogroup nitrogen atoms on the 4-CY molecules in the two adjacent Q[7] cavities (Fig. 4c). Hydrogen bonding between the encapsulated 4-CY molecule and the host Q[7] is evident: the carbon atoms on the benzene ring (C46, C48) form a hydrogen bond with the carbonyl atoms (C37, O12, O14) of the Q[7] host with a C(46)–H···O(14) distance of 2.850(5) Å, C(48)–H···O(12) distance of 2.801(5) Å and a C(48)–H···C(37) distance of 2.765(7) Å. Moreover, the hydrogen-bonding interactions between the oxygen atom (O15) of the hydroxyl group with the portal carbonyl oxygen atom (O12) of Q[7] exhibit distances of O(15)–H···O(12) 1.929(5) Å. Two 4-CY molecules are located outside the Q[6] cavity and form O(C)–H···Cl contacts with $[ZnCl_4]^{2-}$ anions *via* ion-dipole interactions or interact with the outer surface of the Q[7] *via* hydrogen bonding (Fig. 4d).

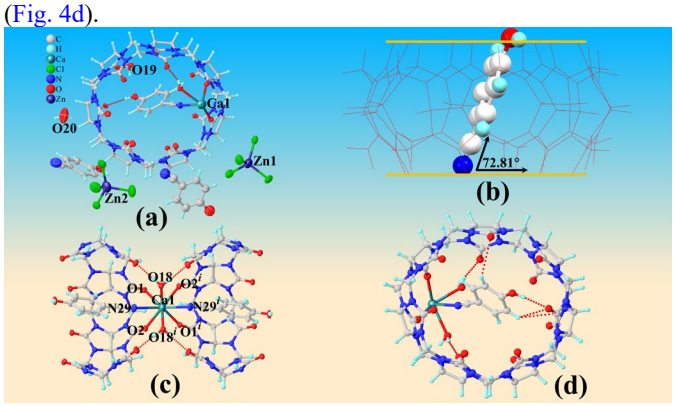

Fig. 4. (a) Asymmetric unit of the complex; (b) the positional relationship between 4-CY and Q[7] host; (c) showing the coordination about Ca1; (d) hydrogen-bonding interactions between the guest molecule and Q[7] host.

Further analysis of the crystal structure of the complex reveals extensive hydrogen bonding between the different complexes. In Fig. 5a, the methine or methylene groups at the outer surface of the Q[7] host form numerous C–H···O hydrogen bonds with carbonyl oxygens of the neighboring Q[7] host, the bond lengths of these hydrogen bonds are between 2.384 (6) and 2.698 (6) Å. Meanwhile, the water molecule O19 is linked with the neighboring Q[7] host through hydrogen bonds, these hydrogen bonds, namely O(19)–H···O(13), O(19)–H···O(14)^{i}, O(19)–H···C(41)^{i}, have bond lengths of 1.802(6), 1.825(5), 2.818(7) Å, respectively, where i = 1−x, +y, 1−z. In addition, the two 4-CY molecules that are located outside the Q[7] cavity interact with the outer surface of the Q[7] *via* hydrogen bonding, or *via* ion-dipole with the $[ZnCl_4]^{2-}$ anion (Fig. 5b). It is worth mentioning that in the complex, the $[ZnCl_4]^{2-}$ anions form C(O)–H···Cl contacts with Q[7], 4-CY molecules or water molecules through ion-dipole interactions (Fig. 5c). Each inclusion complex Q[7]@4-CY is surrounded by five tetrahedral $[ZnCl_4]^{2-}$ counterions (Fig. 6b). As a result, driven by these weak interactions (hydrogen bonding and ion-dipole interactions), the complex constructs a new Q[7]-based QSF framework material (Q[7]-(4-CY)-$[ZnCl_4]^{2-}$-Ca^{2+}), which exhibits a supramolecular structure due to its rich building units. Fig. 6a shows that the complex forms a layered supramolecular structure along the *a*-axis, in which $[ZnCl_4]^{2-}$ anions and 4-CY molecules are arranged regularly between layers. Interestingly, a Chinese knot-like two-dimensional supramolecular structure is observed in the crystal stacking diagram of the parallel cell *ab*-plane of the complex (Fig. 6c).

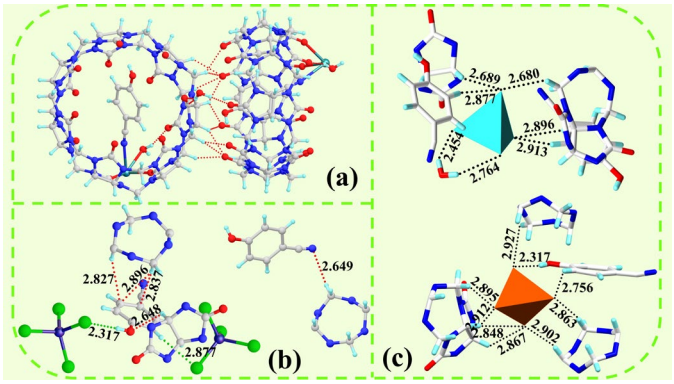

Fig. 5. (a) Hydrogen-bonding interactions between the Q[7]@4-CY; (b) detailed weak interactions of 4-CY molecules; (c) ion-dipole interaction between the $[ZnCl_4]^{2-}$ and Q[7].

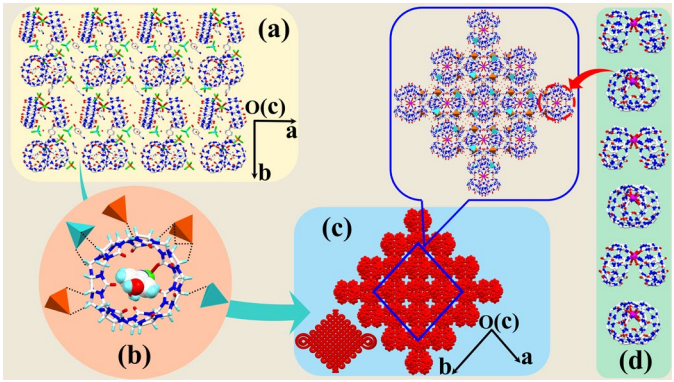

Fig. 6. (a) Two-dimensional structure of complex viewed down the *a* axis; (b) detailed ion-dipole interaction between Q[7]@4-CY and $[ZnCl_4]^{2-}$ anions; (c) two-dimensional structure of complex viewed down the *c* axis.

The density function theory (DFT) calculations are based on Gaussian 16 software package. Under the dispersion-corrected B3lyp-D3 function, the 6-311G(d,p) basis set is used for geometric optimization and energy of the model. The calculation of the composite structure was carried out under the solvation model based on density (SMD) model. Fig. 7 present the simulated UV spectrum, which is consistent with the experimental results. According to DFT calculations, for the synthesized complex, the highest occupied molecular orbital (HOMO) was -6.39 eV (Fig. 8a), the lowest unoccupied molecular orbital (LUMO) was -1.22eV (Fig. 8b). The electrostatic surface potential (ESP) distribution was calculated as shown in Fig. S2. The calculated dipole moment was 6.37 Debye (Fig. S3).

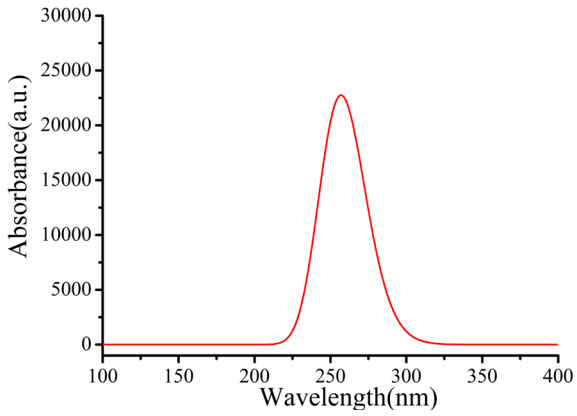

Fig. 7. Simulated UV spectrum of complex.

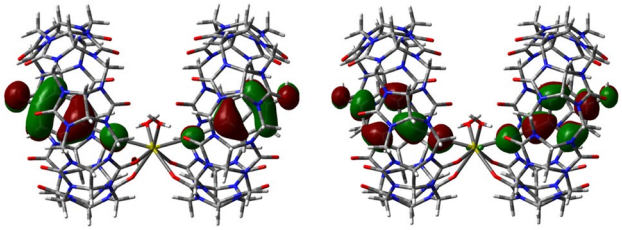

(a) HOMO (-6.3866 eV) (b) LUMO (-1.2169 eV)

Fig. 8. Frontier orbitals of the complex: (a) HOMO, (b) LUMO.

5. Conclusion

In summary, we have investigated the binding interaction between 4-cyanophenol and Q[7] both in the solid state and in aqueous solution. Characterization methods including by ^{1}H NMR spectroscopy, UV-vis absorption spectroscopy, fluorescence spectroscopy and X-ray crystallography, which indicated that Q[7] and 4-CY formed a 1:1 host and guest type complex in solution. Moreover, the crystal structure in the solid state was constructed by Q[7] and 4-CY in the presence of $[ZnCl_4]^{2-}$ and Ca^{2+} as the structure-directing agent in aqueous HCl solutions. The resulting complex forms a stable Q[7]-based supramolecular framework under multiple driving forces, including hydrogen bonding, C-H···π, π···π and ion-dipole interactions.

Table 1. Crystallographic data for complex.

	Complex Q[7]@4-CY
Formula	$C_{126}H_{126}CaCl_{16}N_{62}O_{40}Zn_4$
FW (g·mol^{-1})	4017.64
Crystal system	tetragonal
Space group	*P*-42$_1$*c*
T (K)	273.15
λ (Å)	0.71073
a (Å)	24.077
b (Å)	24.077
c (Å)	32.472
α (°)	90
β (°)	90
γ (°)	90
V (Å^3)	18824.8
Z	4
D_{calcd} (g/cm^3)	1.418
μ (mm^{-1})	0.842
F(000)	8192.0
θ range (°)	2.27-25.027
Reflections collected/unique	539902/16630
R_{int}	0.1808
Data/restraints/parameters	16630/340/1120
Goodness-of-fit on F^2	1.028
R_1, wR_2 [$I > 2\sigma(I)$]	0.0557, 0.1388
R_1, wR_2 (all data)	0.0889, 0.1619
Largest diff.Peak and hole(e.Å^{-3})	0.42/-0.29

Declaration of Competing Interest

The authors declare that they have no known competing financial interests or personal relationships that could have appeared to influence the work reported in this paper.

Acknowledgments

This work was supported by the National Natural Science Foundation of China (No.21871064) and the Technology Fund of Guizhou Province (No. 2018-5781). CR thanks the University of Hull for support.

References

[1]. L. Jason, M. Pritam, C. Sriparna, L. Isaacs, The Cucurbit[*n*]uril Family, Angew. Chem. Int. Ed. 44 (2005) 4844-4870.

[2]. X. L. Ni, X. Xiao, H. Cong, Q. J. Zhu, S. F. Xue, Z. Tao, Self-Assemblies Based on the "Outer-Surface Interactions" of Cucurbit[*n*]urils: New Opportunities for Supramolecular Architectures and Materials, Acc. Chem. Res. 47 (2014) 1386-1395.

[3]. C. Sun, Z. Y. Wang, L. D. Yue, Q. X. Huang, Q. Cheng, R. B. Wang, Supramolecular Induction of Mitochondrial Aggregation and Fusion, J. Am. Chem. Soc. 142 (2020) 16523-16527.

[4]. H. Wu, J. Zhao, X. N. Yang, D. Yang, L. X. Chen, C. Redshaw, L. G. Yang, Z. Tao, X. Xiao, A cucurbit[8]uril-based probe for the detection of the pesticide tricyclazole, Dyes and Pigments 199 (2022) 110076.

[5]. T. Jiang, X. Wang, J. Wang, G. P. Hu, X. Ma, Humidity- and Temperature-Tunable Multicolor Luminescence of Cucurbit[8]uril-Based Supramolecular Assembly, ACS Appl. Mater. Interfaces 11 (2019) 14399-14407.

[6]. P. H. Shan, J. H. Hu, M. Liu, Z. Tao, X. Xiao, C. Redshaw, Progress in host-guest macrocycle/pesticide research: Recognition, detection, release and application, Coordination Chemistry Reviews 467 (2022) 214580.

[7]. Y. Luo, W. Zhang, M. Liu, J. Zhao, Y. Fan, B. Bian, Z. Tao, X. Xiao, A supramolecular fluorescent probe based on cucurbit[10]uril for sensing the pesticide dodine, Chinese Chem. Lett. 32 (2021) 367-370.

[8]. M. Liu, R. Cen, J. S. Li, Q. Li, Z. Tao, X. Xiao, L. Isaacs, Double-Cavity Nor-Seco-Cucurbit[10]uril Enables Efficient and Rapid Separation of Pyridine from Mixtures of Toluene, Benzene, and Pyridine, Angew. Chem. Int. Ed. 61 (2022) e202207209.

[9]. K. Kim, N. Selvapalam, Y. H. Ko, K. M. Park, D. Kim, J. Kim, Functionalized cucurbiturils and their applications, Chem. Soc. Rev. 36 (2007) 267-279.

[10]. R. N. Dsouza, U. Pischel, W. M. Nau, Fluorescent Dyes and Their Supramolecular Host/ Guest Complexes with Macrocycles in Aqueous Solution, Chem. Rev. 111 (2011) 7941-7980.

[11]. S. W. Guo, Q. X. Huang, Y. Chen, J. W. Wei, J. Zheng, L. Y. Wang, Y. T. Wang, R. B. Wang, Synthesis and Bioactivity of Guanidinium-Functionalized Pillar[5]arene as a Biofilm Disruptor, Angew. Chem. Int. Ed. 60 (2021) 618-623.

[12]. R. Cen, M. Liu, J. H. Lu, W. F. Zhang, J. J. Dai, X. Zeng, Z. Tao, X. Xiao, Synthesis and characterization of a sensitive and selective Fe^{3+} fluorescent sensor based on novel sulfonated calix[4]arene-based host-guest complex, Chinese Chem. Lett. 33 (2022) 2469-2472.

[13]. R. L. Lin, J. X. Liu, K. Chen, C. Redshaw, Supramolecular chemistry of substituted cucurbit[*n*]urils, Inorg. Chem. Front. 7 (2020) 3217-3246.

[14]. Y. Luo, W. Zhang, Q. Ren, Z. Tao, X. Xiao, Highly Efficient Artificial Light-Harvesting Systems Constructed in Aqueous Solution Based on Twisted Cucurbit[14]uril, ACS Appl. Mater. Interfaces 14 (2022) 29806-29812.

[15]. X. L. Ni, X. Xiao, H. Cong, L. L. Liang, K. Cheng, X. J. Cheng, N. N. Ji, Q. J. Zhu, S. F. Xue, Z. Tao, Cucurbit[*n*]uril-based coordination chemistry: from simple coordination complexes to novel poly-dimensional coordination polymers, Chem. Soc. Rev. 42 (2013) 9480-9508.

[16]. D. Yang, M. Liu, X. Xiao, Z. Tao, C. Redshaw, Polymeric self-assembled cucurbit[*n*]urils: Synthesis, structures and applications, Coordin. Chem. Rev. 434 (2021) 213733.

[17]. W. Zhang, Y. Luo, J. Zhao, C. Zhang, X. L. Ni, Z. Tao, X. Xiao, Controllable fabrication of a supramolecular polymer incorporating twisted cucurbit[14]uril and cucurbit[8]uril *via* self-sorting, Chinese Chem. Lett. 33 (2022) 2455-2458.

[18]. X. Yang, R. Wang, A. Kermagoret, D. Bardelang, Oligomeric Cucurbituril Complexes: from Peculiar Assemblies to Emerging Applications, Angew. Chem. Int. Ed. 59 (2020) 21280-21292.

[19]. P. H. Shan, R. L. Lin, M. Li, Z. Tao, X. Xiao, J. X. Liu, Recognition of Glycine by Cucurbit[5]uril and Cucurbit[6]uril: A Comparative Study of Exo- and Endo- Binding, Chinese Chem. Lett. 32 (2021) 2301-2304.

[20]. R. J. Fernandes, P. Remón, A. J. Moro, A. Seco, A. S. D. Ferreira, U. Pischel, N. Basílio, Toward Light-Controlled Supramolecular Peptide Dimerization, J. Org. Chem. 86 (2021) 8472-8478.

[21]. S. Garain, B. C. Garain, M. Eswaramoorthy, S. K. Pati, S. J. George, Light-Harvesting Supramolecular Phosphors: Highly Efficient Room Temperature Phosphorescence in Solution and Hydrogels. Angew. Chem. Int. Ed. 60 (2021) 19720-19724.

[22]. L. Isaacs, Stimuli responsive systems constructed using cucurbit[*n*]uril-Type molecular containers, Acc. Chem. Res. 47 (2014) 2052-2062.

[23]. A. E. Kaifer, Toward reversible control of cucurbit[*n*]uril complexes, Acc. Chem. Res. 47 (2014) 2160-2167.

[24]. R. H. Gao, L. X. Chen, K. Chen, Z. Tao, X. Xiao, Development of hydroxylated cucurbit[*n*]urils, their derivatives and potential applications, Coordin. Chem. Rev. 348 (2017) 1-24.

[25]. J. Tian, H. Wang, D. W. Zhang, Y. Liu, Z. T. Li, Supramolecular organic frameworks (SOFs): homogeneous regular 2D and 3D pores in water, Natl. Sci. Rev. 4 (2017) 426-436.

[26]. Y. Huang, R. H. Gao, M. Liu, L. X. Chen, X. L. Ni, X. Xiao, H. Cong, Q. J. Zhu, K. Chen, Z. Tao, Cucurbit[*n*]uril-Based Supramolecular Frameworks Assembled through Outer-Surface Interactions, Angew. Chem. Int. Ed. 60 (2021) 15166-15191.

[27]. J. Tian, L. Chen, D. W. Zhang, Y. Liu, Z. T. Li, Supramolecular organic frameworks: engineering periodicity in water through host-guest chemistry, Chem. Commun. 52 (2016) 6351-6362.

[28]. W. T. Xu, Y. Luo, W. W. Zhao, M. Liu, G. Y. Luo, Y. Fan, R. L. Lin, Z. Tao, X. Xiao, J. X. Liu, Detecting Pesticide Dodine by Displacement of Fluorescent Acridine from Cucurbit[10]uril Macrocycle, J. Agric. Food Chem. 69 (2021) 584-591.

[29]. M. Liu, L. X. Chen, P. H. Shan, C. J. Lian, Z. H. Zhang, Y. Q. Zhang, Z. Tao, X. Xiao, Pyridine Detection Using Supramolecular Organic Frameworks Incorporating Cucurbit[10]uril, ACS Appl. Mater. Inter. 13 (2021) 7434-7442.

[30]. K. Kim, Mechanically interlocked molecules incorporating cucurbituril and their supramolecular assemblies, Chem. Soc. Rev. 31 (2002) 96-107.

[31]. X. L. Zhang, X. L. Liu, X. Y. Sang, S. R. Sheng, Poly (ethylene glycol)-bound sulfonyl chloride as an efficient catalyst for transformation of aldoximes to nitriles, Synthetic Commun. 47 (2017) 232-237.

[32]. P. Przybylski, G. Wojciechowski, B. Brzezinski, G. Zundel, F. Bartl, FTIR studies of the interactions of 1, 3, 5-triazabicyclo [4. 4. 0] dec-5-ene with 4-tert-butylphenol and 4-cyanophenol, J. Mol. Struct. 661 (2003) 171-182.

[33]. J. Kim, I. S. Jung, S. Y. Kim, E. Lee, J. K. Kang, S. Sakamoto,

K. Yamaguchi, K. Kim, New Cucurbituril Homologues: Syntheses, Isolation, Characterization, and X-ray Crystal Structures of Cucurbit[*n*]uril (n = 5, 7, and 8), J. Am. Chem. Soc. 122 (2000) 540-541.

[34]. G. M. Sheldrick, SADABS: Program for Empirical Absorption Correction of Area Detector Data. University of Göttingen, Germany. 1996.

[35]. G. M. Scheldrick, SHELXT-Integrated space-group and crystals-structure determination, Acta Cryst. 71 (2015) 3-8.

[36]. O. V. Dolomanov, L. J. Bourhis, R. J. Gildea, J. A. K. Howard, H. Puschmann, OLEX2: a complete structure solution, refinement and analysis program, J. Appl. Cryst. 42 (2009) 339-341.

[37]. A. L. Spek, PLATON SQUEEZE: a tool for the calculation of the disordered solvent contribution to the calculated structure factors, Acta Cryst. 71 (2015) 9-18.

[38]. T. Jiang, X. Wang, J. Wang, G. P. Hu, X. Ma, Humidity- and temperature-tunable multicolor luminescence of cucurbit[8]uril-based supramolecular assembly, ACS Appl. Mater. Interfaces. 11 (2019) 14399-14407.